Chemistry–A European Journal
Research Article
doi.org/10.1002/chem.202300720
Chemistry Europe
European Chemical Societies Publishing
www.chemeurj.org

The Role of the Amino Acid Molecular Characteristics on the Formation of Fluorescent Gold- and Silver-Based Nanoclusters

Rita Bélteki,[a] Loretta Kuklis,[a] Gyöngyi Gombár,[a] Ditta Ungor,[a] and Edit Csapó*[a, b]

Abstract: Role of amino acids like *L*-phenylalanine (Phe), *L*-glutamine (Gln) and *L*-arginine (Arg) is described and interpreted in terms of their potential for preparation of fluorescent molecular-like gold and silver nanostructures. We are among the first to demonstrate the effect of syntheses conditions as well as the molecular characteristics of Phe, Gln and Arg amino acids on the structure of the formed products. Comprehensive optical characterizations (lifetime, quantum yield (QY%)) of the blue-emitting products were also carried out. It was confirmed that for all Au-containing samples and for Gln-Ag system the characteristic fluorescence originates from few-atomic metallic nanoclusters (NCs) where the reduction of metal ions was promoted by citrate in some cases. Relatively high QY% (~18%) was obtained for Arg-stabilized Au NCs due to the existence of an electrostatic interaction between the electron rich, positively charged guanidium side chain of Arg and the negatively charged carboxylate group of citrate on the metallic surface. Size and structural analysis of the products were evaluated by infrared measurements and dynamic light scattering techniques.

Introduction

Metallic nanostructures functionalized with amino acids, peptides and proteins, especially those based on noble metals, are playing an increasingly important role in both materials science and life sciences due to their diverse structural and optical properties.[1,2] The classic noble metal nanoparticles (NPs) having size larger than 2–3 nm show plasmonic features based on the localized surface plasmon resonance (LSPR) phenomena.[1] In addition to NPs, nanoclusters (NCs) are gaining ground, which are much smaller in size ($d < 2$ nm) and therefore exhibit different optical properties, which is the size- and structure-dependent photoluminescence (PL).[3] Several synthesis protocols are used all around the world to synthesize noble metal NCs such as microwave-assisted, sonochemical, photoreductive, etching-based, kinetically-controlled or template-assisted syntheses.[3] Because of the application of NCs in biomedical fields, the latter is increasingly preferred, where proteins or peptides, used in large excess, perform the function of a template.[4] Numerous proteins like human or bovine serum albumin,[5] lysozyme,[6] globulins[7] *etc.* have been applied previously for fabrication of protein-stabilized Au and Ag NCs, but the number of articles relating to the presentation of template-assisted synthesis protocols of noble metal NCs by using amino acids is relatively less.[4] In the case proteins consisting of amino acids, it is not clear exactly which amino acid(s) play a dominant role in the reduction of metal ions and the stabilization of the metal core, so it is particularly important to explore the above mentioned role of individual amino acids. Depending on the concentration of the precursor metal ions, the ratio of the amino acid/metal ions and the reaction temperature the direct interaction of *L*-histidine (His), *L*-tyrosine (Tyr), *L*-proline (Pro), *L*-tryptophane (Trp) and *L*-methionine (Met) with $[AuCl_4]^-$ results in the formation of Au NCs which possess intense blue PL, except of Met, where the NCs show yellow emission.[4] For *L*-cysteine (Cys) the formation of a well-known and widely characterized self-assembled coordination polymeric structure is confirmed by X-ray diffraction (XRD) and small-angle X-ray scattering (SAXS) techniques.[8]

Besides these amino acids, only 4–5 articles have been published for the fabrication of Au, Ag or Cu NCs – in addition to the results of plasmonic nanoparticles (NPs) – by using *L*-phenylalanine (Phe),[9] *L*-arginine (Arg)[10] and *L*-glutamine (Gln),[11] but the majority of these either interpret the structure of NCs in a theoretical way and do not include experimental results at all, or are incomplete in the interpretation of the effect of experimental conditions on cluster formation. To the best of our knowledge, in case of Gln only one article focuses on Density Functional Theory (DFT) computations of the

[a] R. Bélteki, L. Kuklis, G. Gombár, Dr. D. Ungor, Dr. E. Csapó
MTA-SZTE Lendület "Momentum"
Noble Metal Nanostructures Research Group
University of Szeged
Rerrich B. sqr. 1, 6720, Szeged (Hungary)
E-mail: juhaszne.csapo.edit@med.u-szeged.hu

[b] Dr. E. Csapó
Interdisciplinary Excellence Center
Department of Physical Chemistry and Materials Science
University of Szeged
Rerrich B. sqr. 1, H-6720, Szeged (Hungary)
E-mail: juhaszne.csapo.edit@med.u-szeged.hu
Homepage: https://csapoedit.hu/
https://scholar.google.hu/citations?user=ealcbLQAAAAJ&hl=hu

Supporting information for this article is available on the WWW under https://doi.org/10.1002/chem.202300720

molecular and physical features of Gln-templated noble metal NCs without the presentation of any experimental data.[11] For Arg two articles have been reported on NCs, where the Arg was used as surface functionalizing ligand for the pre-synthesized 6-Aza-2-thiothymine (ATT)-reduced Au NCs.[10,12] There are two articles in the literature for Phe-reduced Au[13] and Cu NCs,[9] but for gold-containing, the experimental data are inconsistent in interpreting the fluorescence property,[13] while for copper-based NCs, the reduction of metal ions was promoted by hydrazine.[9]

Based on these findings, in this work we aim to study the direct interaction of Phe, Arg, and Gln with $[AuCl_4]^-$ and Ag^+ -ions by varying several experimental conditions like amino acid/metal ion molar ratio, concentration of the metal ions, pH, temperature and reaction time to give new experimental data on the effect of these amino acids on noble metal nanocluster formation and to complement the existing literature. Where the formation of fluorescent product was negligible, the effect of Na-citrate as further mild reducing agent was also studied on the cluster's synthesis. The detailed optical characteristics of the purified fluorescent products were also carried out and the data were interpreted. The results of optical studies were supported by Fourier-transform infrared (FTIR) spectroscopy and dynamic light scattering (DLS) experiments, where the opportunity has arisen.

Results and Discussion

Optimization of the preparation protocols

To study the effect of several experimental factors on the formation of fluorescent products, all systems consistently followed a single test protocol. In a first step, the amino acid/metal ion molar ratio was optimized, followed by the adjustment of the metal ion concentration. Next, the effect of pH was studied, followed by the role of the temperature and reaction time. The results are presented in this order for all systems.

Phe-reduced Au and Ag nanostructures

A. Amiri Sadeghan et al. published that[13] the interaction of Phe with $[AuCl_4]^-$ ions results in the formation of Phe-stabilized Au NCs using Phe:$[AuCl_4]^-$/2:1 molar ratio after 4 h reaction time at 60 °C, when the pH was adjusted to pH = 6.0. After the synthesis the sample showed dark yellow color. Our studies did not confirm these experimental results. Moreover, the PL feature of their product did not support; no emission spectrum was presented in the article.[13] Most probably the formation of plasmonic NPs instead of NCs is feasible under these conditions. Figure 1(A) clearly shows that higher amino acid excess results in the formation of fluorescent Au-and Ag-based nanostructures. For Au the maximum PL intensity was obtained at Phe:$[AuCl_4]^-$/20:1 molar ratio, while in case of silver-based systems the samples prepared at Phe:Ag^+/80:1 molar ratio result in the highest PL intensity. The metal ion concentrations

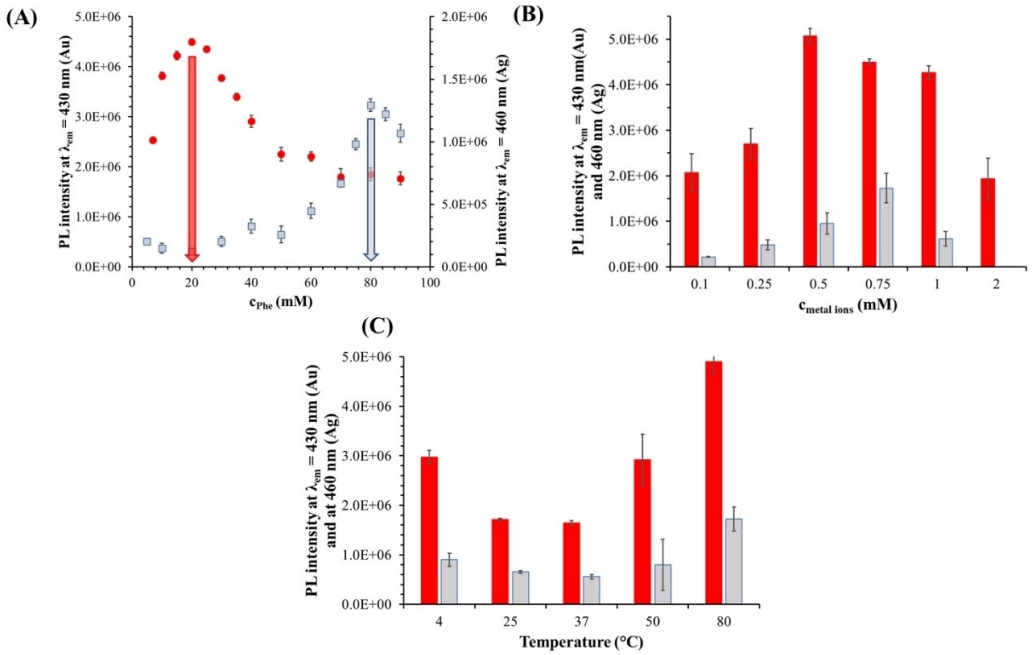

Figure 1. A) PL intensity of the Au- (red) and Ag-based (grey) systems as a function of $c_{Phe.}$ ($c_{metal\ ions}$ = 1.0 mM, T = 80 °C, pH(Au) = 10.0, pH(Ag) = 11.0, t = 6 day). B) PL intensity of the Au- (red) and Ag-based (grey) systems as a function of $c_{metal\ ions.}$ (Phe:$[AuCl_4]^-$/20:1; (Phe:Ag^+/80:1, T = 80 °C, pH(Au) = 10.0, pH(Ag) = 11.0, t = 6 day). C) PL intensity of the Au- (red) and Ag-based (grey) systems as a function of temperature. (Phe:$[AuCl_4]^-$/20:1; (Phe:Ag^+/80:1, c_{AuCl4-} = 0.5 mM, c_{Ag+} = 0.75 mM, pH(Au) = 10.0, pH(Ag) = 11.0, t = 6 day). ($\lambda_{ex(Au)}$ = 370 nm, $\lambda_{ex(Ag)}$ = 365 nm).

also have a significant effect on the formation of nanoclusters. Based on the results presented on Figure 1(B), it was confirmed that the $c_{AuCl4-} = 0.50$ mM and $c_{Ag+} = 0.75$ mM values are optimal for syntheses. Application of higher metal ion concentration already favours the NPs formation, as it was confirmed previously.[14]

As a next step, the syntheses have been carried out at different pH values (Figure S1) in the range from pH = 2.0 to pH = 12. It was obtained that below pH ~ 8.0 no products having PL property was formed. If the pH reached the pH ~ 9.0 measurable PL was detected which was increased with increasing pH. The highest PL intensity was reached at pH ~ 10.0–11.0, which is in good agreement with literature data.[5,7] Consequently, pH ~ 10.0–11.0 was selected as ideal pH for synthesis, where the functional groups of the Phe are all deprotonated[15] and the reducing ability is much stronger. The reaction temperature is also an important factor to produce PL products with high yield (%). The reactions have been repeated at various temperature values (Figure 1C) as well, but for both cases the 80 °C seemed to be appropriate. Higher temperatures shift the reaction towards the formation of plasmonic particles, and slight aggregation is observed, so a value of 80 °C was adopted. For reaction time, the maximum PL intensity is observed after 6 and 14 days in Au- and Ag- systems, respectively. In summary, the interaction of the two studied noble metal ions with Phe under similar experimental conditions (pH, temperature (Figure 1C), metal ion concentration (Figure 1B)) results in a fluorescent product, but a lower ligand excess (Figure 1A) and shorter reaction time are also appropriate for gold. In the case of silver, despite the higher ligand excess and longer incubation time, the system may still contain unreduced Ag^+ ions based on the iodide ion reaction performed.

Arg-reduced Au and Ag nanostructures

By replacing the aromatic side chain of the amino acid with an electron-rich guanidinium group, the molecular structure changes, which may indicate a different degree of interaction with gold(III)- and silver(I)ions. The interactions of Arg amino acid with $[AuCl_4]^-$ and Ag^+ ions also result in the formation of blue emitting nanostructures, but the optimization of the experimental conditions is required. As it can be seen on Figure 2(A) higher concentration of Arg is necessary to achieve adequate fluorescence. The application of extreme high ligand excess is well-known in the literature to produce fluorescent NCs, which ensures the appropriate reduction of metal ions, the stabilization of the clusters formed and the formation of surface functional groups. For example, in the work of X. Mu and co-workers, the preparation of a *L*-proline-stabilized Au NCs were presented, where the molar ratio of the amino acid and the precursor Au(III) salt was proline:$[AuCl_4]^-$/830:1.[16] Their synthesized Au NCs showed blue-emission ($\lambda_{em} = 440$ nm) using 365 nm as excitation wavelength. The QY% was ca. 3%.[16] In case of our gold-containing sample the highest PL can be reached at Arg:$[AuCl_4]^-$/800:1 molar ratio, while the use of Arg:

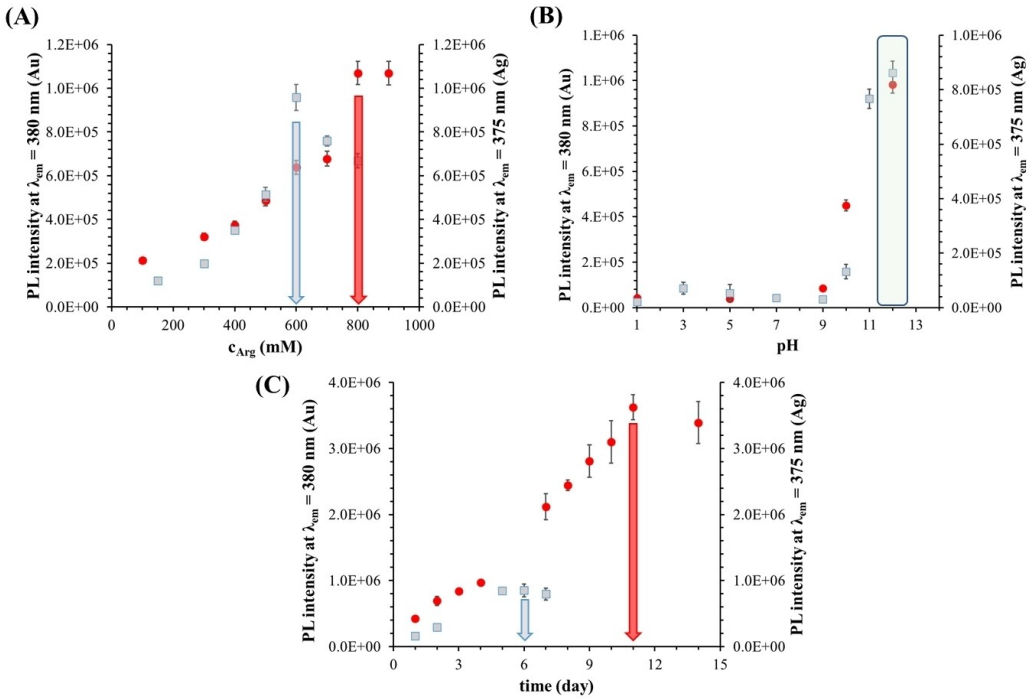

Figure 2. A) PL intensity of the Au- (red) and Ag-based (grey) systems as a function of $c_{Arg.}$ ($c_{metal\ ions} = 1.0$ mM, T = 80 °C, pH = 12.0, $t = 6$ day). B) PL intensity of the Au- (red) and Ag-based (grey) systems as a function of pH (Arg:$[AuCl_4]^-$/800:1; (Arg:Ag^+/600:1, $T = 80$ °C, $c_{AuCl4-} = 1.0$ mM; $c_{Ag+} = 1.50$ mM, $t = 6$ day). C) PL intensity of the Au- (red) and Ag-based (grey) systems as a function of incubation time (Arg:$[AuCl_4]^-$/800:1; (Arg:Ag^+/600:1, $c_{AuCl4-} = 1.0$ mM, $c_{Ag+} = 1.50$ mM, pH = 11.0, $t = 6$ day). ($\lambda_{ex(Au)} = 310$ nm, $\lambda_{ex(Ag)} = 305$ nm).

Ag^+ /600:1 molar ratio result in fluorescent products with the highest intensity.

A comparison of the two systems shows that fluorescence products having extremely weak PL are formed in the case of gold, so Na-citrate was also used as an additional mild reducing agent, with a ratio of Na-citrate:$[AuCl_4]^-$/5:1 to promote the complete reduction of metal ions. By using citrate, the formation of colloidal particles with plasmonic property could be observed after one day incubation time which was removed from the dispersion. Because of the application of citrate, the formation of clusters containing Au^0 is strongly preferred. For Arg/Ag^+ system the application of Na-citrate was not justified because fluorescent products with intense PL intensity was formed and thus presumably, the characteristic fluorescence in the two systems is due to different structures. It can be concluded that the change of the aromatic moiety to guanidium group containing aliphatic-N donors is not favorable to the reduction of metal ions thus the application of high amino acid excess can be explained. As it was shown in the previous chapter for Phe-containing systems (Figure 1B), the choice of the right metal ion concentration is also important for the formation of fluorescent products with high yield and maximum intensity. Based on this, the optimum concentration was found to be $c_{AuCl4-} = 1.0$ mM and $c_{Ag+} = 1.5$ mM. In case of pH (Figure 2B) it was confirmed that the basic condition (pH = 12.0) is particularly favorable for the formation of clusters for the reasons mentioned for Phe. Temperature and reaction time were also optimized as additional experimental parameters. The reactions have been repeated at various temperature values as well, but for both cases we obtained that increasing the temperature has a positive effect on the formation of products; the 80 °C seemed to be appropriate as it was also applied for Phe-containing samples (Figure 1C). In case of reaction time (Figure 2C), we confirmed that the maximum PL intensity is observed after 11 and 6 days for gold and silver-containing systems, respectively. Overall, it can be concluded that the interaction of metal ions with Arg (without the addition of other reducing agents) leads to the formation of a product with more intense fluorescence in the Ag-containing system, and a significantly shorter incubation time is sufficient. In the case of gold, the addition of citrate promotes the formation of clusters with high PL intensity. The effects of temperature, metal ion concentration and pH are almost similar for both systems.

Gln-reduced Au and Ag nanostructures

The side chain of Gln amino acid contains an amide functional group, which means significantly less *N*-donor than the guanidium moiety of Arg and thus suggests a weaker reducing capacity as well by default. The direct interaction of Gln with $[AuCl_4]^-$ and Ag^+ ions does not result in the appearance of PL products even with the use of large excess ligands. Based on this experimental result, as a next step, we studied the effect of the combined use of Gln and Na-citrate on the formation of products. As the Figure 3(A) shows under the application of larger citrate concentration (100 mM for Au, 280 mM for Ag) excess measurable less amino acid excess is required than in

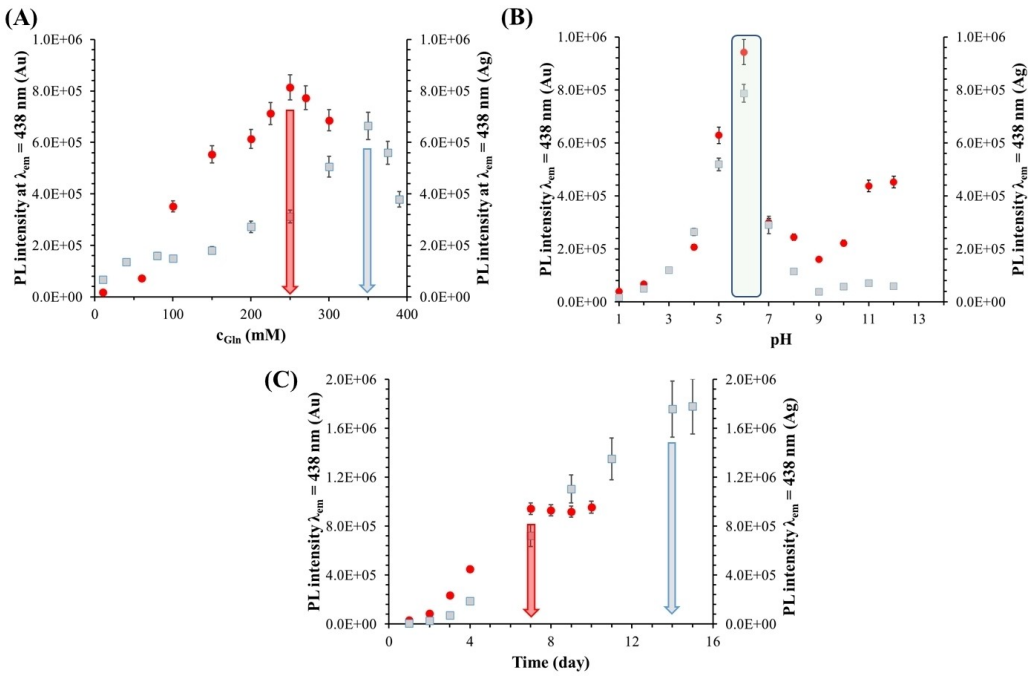

Figure 3. A) PL intensity of the Au- (red) and Ag-based (grey) systems as a function of $c_{Gln.}$ ($c_{metal\ ions} = 1.0$ mM, $T = 80$ °C, pH = 6.0, $t = 6$ day). B) PL intensity of the Au- (red) and Ag-based (grey) systems as a function of pH (Gln:$[AuCl_4]^-$/250:1; (Gln:Ag^+/350:1, $T = 80$ °C, $c_{metal\ ions} = 1.0$ mM; $t = 6$ day). C) PL intensity of the Au- (red) and Ag-based (grey) systems as a function of incubation time (Gln:$[AuCl_4]^-$/250:1; (Gln:Ag^+/350:1, $c_{metal\ ions} = 1.0$ mM, pH = 6.0, $t = 6$ day). In all cases the $\lambda_{ex} = 350$ nm.

case of Arg. Namely, the highest PL intensity is obtained at Gln:$[AuCl_4]^-$/250:1 and Gln:Ag^+/350:1 amino acid:metal ion molar ratios (Figure 3A).

For metal ion concentration and reaction temperature no significant changes were observed; $c = 1.0$ mM and $T = 80\,^{\circ}C$ were applied for both systems. In case of pH an interesting effect is observed, which is presented on Figure 3(B). For both metal ions the PL products having highest intensity were formed at pH ~ 6.0, where the Gln amino acid has neutral charge ($-COO^-/NH_3^+$). In contrast to Phe and Arg systems, in the Gln-containing samples the application of citrate excess greatly facilitates the complete reduction of the metal ions and thus the formation of the metallic structure, and the binding of the protonated amino group (ammonium group/NH_3^+) to the citrate-stabilized negative metallic surface is preferred. In case of incubation time, it can be obtained that for Au-containing sample the PL intensity reaches the highest value after 7 days, while for Ag-based system an incubation period of 14 days was found to be optimal. In summary, we can obtain that the Gln has the weakest reduction property of the 3 amino acids studied. The use of extra citrate strongly supports the formation of NCs containing dominantly Au^0 which was confirmed by the iodide test as well. The application of only citrate does not result in the appearance of fluorescent products at 80 °C, only plasmonic nanoparticles were formed.

Optical characteristics of the prepared system

The first step was to determine the comprehensive optical properties of the purified nanostructures, including the registration of the excitation/emission spectra (Figure S2), and the determination of the absolute quantum yield (QY%) values. It can be noted that among the pure amino acids (Phe, Arg, Gln) only the Phe shows measurable fluorescence due to the aromatic side chain ($\lambda_{em} = 282$ nm) using 240 nm excitation (Figure S3). For Arg and Gln molecules PL emission cannot be detected. Table 1 summarizes the characteristic fluorescence data of the studied systems with the percent of the light utilization using the defined λ_{ex}. It can be generally established that for the use of same amino acid the nanohybrid systems formed in the Au- and Ag -containing samples have similar excitation and emission maxima. The magnitude of the QY% also show a similar tendency. Based on the calculated values, the Arg can facilitate the light utilization to a greater extent perhaps due to the electron rich functional groups in the side chain, because the highest QY% (~15%–18%) can be reached by Arg-containing systems. The stability of the clusters is further increased by the formation of electrostatic salt-bridge between the positively charged guanidinium group ($pK_a = 12.48$) and the negatively charged citrate on the metallic surface. The existence of this interaction may also support the relatively high QY value. Although Phe itself is fluorescent, it does not exhibit any measurable emission property at 370 nm excitation, which further confirms the presence of clusters.

Table 1. The excitation (λ_{ex}) and emission (λ_{em}) maxima with the calculated QY% data of the prepared samples.

Sample	λ_{ex} [nm]	λ_{em} [nm]	QY [%]
Phe/$AuCl_4^-$	370	430	3.31 ± 0.18
Phe/Ag^+	365	460	1.69 ± 0.18
Arg/$AuCl_4^-$	305	380	17.94 ± 0.04
Arg/Ag^+	310	375	14.30 ± 0.27
Gln/$AuCl_4^-$	350	438	6.26 ± 0.10
Gln/Ag^+	350	438	8.30 ± 0.09

Mainly 3 different structures listed below are likely to form depending on the reducing capacity of the selected biomolecules and the applied molar ratios of the amino acids and metal ions:

(i) the biomolecule is not able to reduce the metal salt at all, and the amount of biomolecule is either equivalent to the metal ion or the excess is not significant: the formation of metal complex containing the metal ion in unchanged oxidation state is preferred (e.g., Au(III)-heterocyclic arylacetylide complex;[17]
(ii) if a larger excess of biomolecule is used, the metal ion is partially reduced and forms metal complexes (e.g., Au(I)-(alkynyl-naphthalimide) complex;[18]
(iii) by using relatively high biomolecule excess where the biomolecule a has great reducing capacity as well, the formation of nanoclusters containing the metals in dominantly zero oxidation state is expected.[4]

Considering the preparation conditions (molar ratios, presence of citrate, *etc.*) and the determined emission maxima, all gold-containing systems perhaps are in nanocluster form with metallic behavior. Based on these findings the number of the metal atoms (***N***) in the cluster cores can simply be calculated by the basically accepted Jellium model[19] by knowing the Fermi energy of the bulk metal ($\boldsymbol{E_{Fermi}}$, E_{Fermi} of Au = 5.53 eV and E_{Fermi} of Ag = 5.49 eV) and the energy of the emitted light ($\boldsymbol{E_{emission}}$):

$$N = \left(E_{Fermi}/E_{Emission}\right)^3 \quad (1)$$

Based on the calculation [Equation (1)], it can be estimated that the Phe- and Gln-stabilized Au NCs contain ~7–8 metal atoms, while the Arg-Au NCs build up from ca. 5 Au atoms. Similar to the Au-systems, the Gln/Ag^+ reaction also resulted in the formation of few-atomic Ag NCs, which also contains ca. 7–8 metal atoms in the primer cluster cores. In the other two Ag-containing samples the cluster formation is not preferred. For the deeper investigation of the detected fluorescence, the TCSPC method was selected. The typical decay profiles, as well as the photos of the samples under UV-light ($\lambda_{max} = 365$ nm) are presented in Figure 4. Based on the decay curves, the average lifetimes (τ) are ca. 0.9 and 1.4 ns in the case of Phe-Au and -Ag systems, respectively. In contrast, the application of the positively charged Arg amino acid resulted in longer ~1.6 ns (Au) and ~1.8 ns (Ag) τ values. In the case of Gln-containing systems the Au has 2.9 ns and the Ag has 5.7 ns average τ. The lifetimes in the case of the studied samples show an increasing trend according to the order Phe < Arg < Gln. As it is well-known that beside the oxidation state of the central metal atoms, the chemical nature of the surface ligand has also a

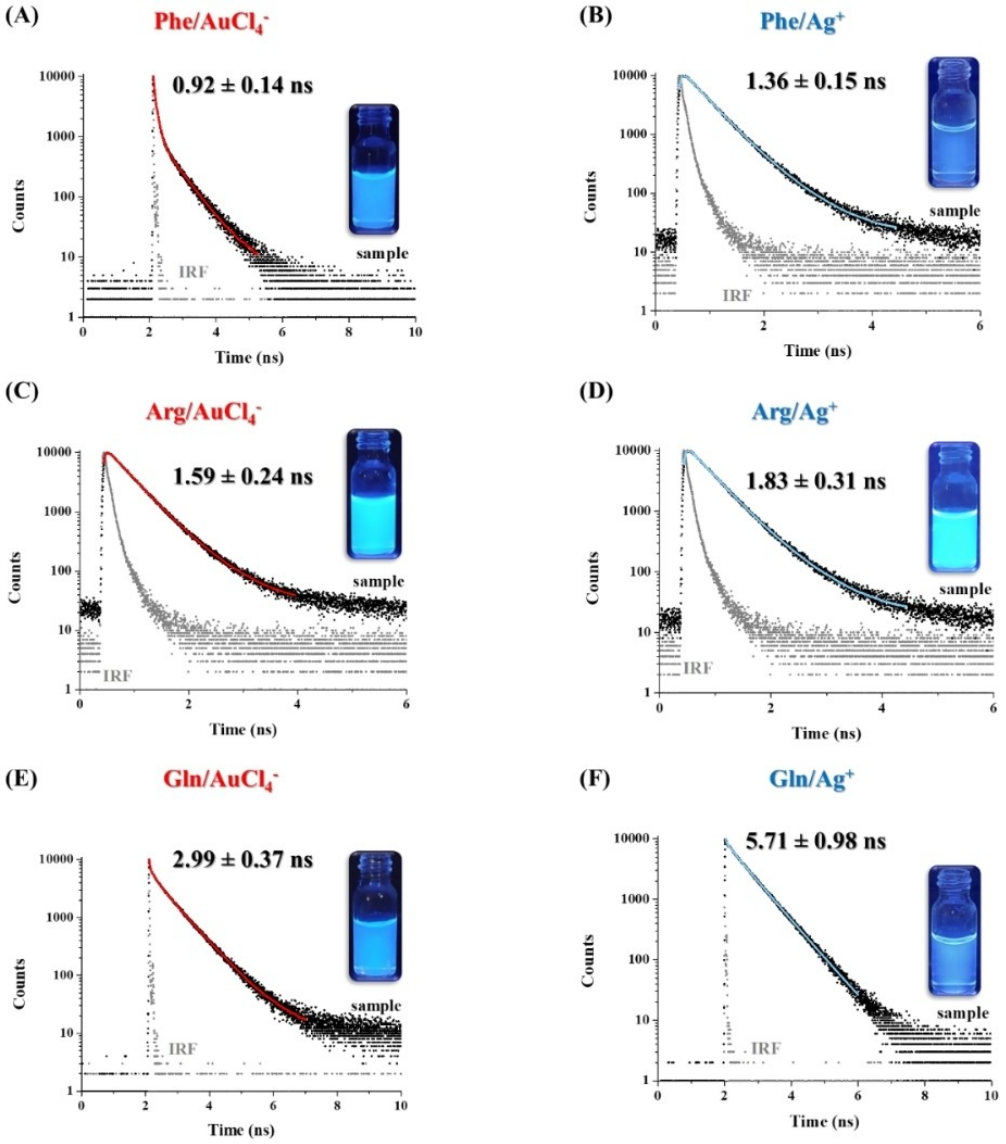

Figure 4. The fluorescence decay profiles with the photos of the samples under UV-lamp (λ_{max} = 365 nm) of the A) $Phe/AuCl_4^-$ (λ_{ex} = 371 nm) and B) Phe/Ag^+ (λ_{ex} = 371 nm), the C) $Arg/AuCl_4^-$ (λ_{ex} = 310 nm) and D) Arg/Ag^+ (λ_{ex} = 310 nm); E) $Gln/AuCl_4^-$ (λ_{ex} = 371 nm) and F) Gln/Ag^+ (λ_{ex} = 371 nm) systems with the average lifetime values. The decay curves were registered at the previously defined emission maxima.

great influence on the average fluorescence lifetime,[20,21] which can provide approximate information about the structure of the prepared systems. Despite the similar atomic numbers in the metal cores, the average fluorescence lifetimes show different values depending on the chosen amino acid. The Phe has aromatic side chain without any special heteroatoms, therefore the electron-attracting or donating effects between the cluster core and surface molecules do not appear dominantly. In contrast, the electron-rich positively charged side chain of Arg amino acid can significantly facilitate the appearance of the *ligand-to-metal* (LMCT) or *ligand-to-metal-metal* (LMMCT) charge transfer. In the case of the Gln, different effect prevails. This molecule has a longer polar, but uncharged side chain with electron-withdrawing moieties, which can form a rigid structure on the surface of ultra-small metallic cores similarly to the sterically hindered polymers.[22] This rigid structure can cause delayed fluorescence, which manifests itself in the longer average lifetime values. For Ag-containing systems, two fluorescent Ag^+ -containing complexes and a metallic Ag NCs can be identified depending on the amino acid and the application of extra citrate. In the case of the Phe-Ag^+ and Arg-Ag^+ similar average values can be determined. In contrast, the application of the Gln with higher amount of citrate resulted the formation of few-atomic Ag NCs, which is proven by the longest, delayed fluorescence. Based on the fitting of every decay profile, three main lifetime components can be separated (Table 2). As data in Table 2 show that, the τ_3 components (*ca.* 0.3 ns) are almost the same in every sample. Since gold and silver have very similar chemical structures, therefore the photons originates from the metal-to-metal charge transfer in

Table 2. The determined lifetime components (τ_1–τ_3) with their contribution percentage and the goodness factor (χ^2) values.

Sample	τ_1 [ns]	τ_2 [ns]	τ_3 [ns]	χ^2
Phe/ $AuCl_4^-$	0.96 ± 0.08 (40.71 %)	5.83 ± 0.10 (43.25 %)	0.27 ± 0.05 (16.04 %)	1.03
Phe/Ag^+	1.28 ± 0.09 (35.43 %)	6.53 ± 0.11 (52.85 %)	0.31 ± 0.02 (11.72 %)	1.12
Arg/ $AuCl_4^-$	2.35 ± 0.23 (19.35 %)	7.35 ± 0.08 (66.65 %)	0.31 ± 0.01 (14.01 %)	1.16
Arg/Ag^+	3.49 ± 0.19 (56.32 %)	6.04 ± 0.24 (31.98 %)	0.35 ± 0.03 (11.70 %)	1.04
Gln/ $AuCl_4^-$	2.68 ± 0.37 (12.12 %)	7.25 ± 0.05 (82.51 %)	0.31 ± 0.02 (5.38 %)	1.02
Gln/Ag^+	2.86 ± 0.91 (5.03 %)	6.91 ± 0.05 (94.42 %)	0.27 ± 0.07 (0.56 %)	1.12

the formed zero valance stated cluster cores (Phe-Au, Gln-Au and Gln-Ag) or the aurophilic (Au···Au)/argentophilic (Ag···Ag) interactions of the metal complexes in the case of Arg-Au, Arg-Ag and Gln-Ag, respectively.[20,23,24] In contrast, both τ_1 and τ_2 are ligand-dependent properties, which show different contribution percentages depending on the selected amino acids and belong to the LMCT and LMMCT, respectively.

Structural characteristics of the prepared systems

For structural characterization FTIR spectra of the nanopowders were registered, and Figure 5. represents the spectra in the range of 1750–1100 cm^{-1} (middle IR), while the Figure S4 shows the all range (4000–1000 cm^{-1}). As a reference, FTIR spectra of the pure amino acids were also recorded at same pH values, thus the differences due to the deprotonation of the functional groups need not be considered. *For Phe-containing samples* (Figure 5A) the dominant shift of the stretching vibrations of the asym. and sym. COO^- (ν_{as} (COO^-), ν_s (COO^-)) and aromatic ring (ν (CC_{ring}) cannot be observed in metal-based systems, which results do not indicate the binding of these functional groups to metal center. In the gold-containing sample the most dominant shift can be found for NH-bending, which is moved from 1552 cm^{-1} to 1572 cm^{-1}, while the ν (C–N) is shifted from 1121 cm^{-1} to 1138 cm^{-1}. Based on these results the presence of amino-N on the metal center is probably. For silver-containing sample the detectable changes of the above-mentioned vibrations cannot be found under the IR measuring conditions. The most striking change compared to pure amino acid is the shift of the β=CH bands at around 1280–1328 cm^{-1} (4 smaller vibration bands), which are observed at 1301–1345 cm^{-1} and their intensities are also changed. Previous results support the dominant presence of unreduced Ag(I) ions in final product. Assuming the formation of an Ag(I)-Phe complex DFT calculations of N. C. Polfer et al.[25] clearly confirmed the dominant presence of a tridentate binding of the amino-N, the carbonyl-O and the π-cloud of the aromatic ring.

For Arg-containing samples (Figure 5B) the IR studies do not provide determinative results. In case of Arg/$AuCl_4^-$ the formation of a metallic surface is supported by the quality (flattening of the characteristic vibration bands) of the IR spectrum. The formation of Arg-Au NCs is also likely due to the

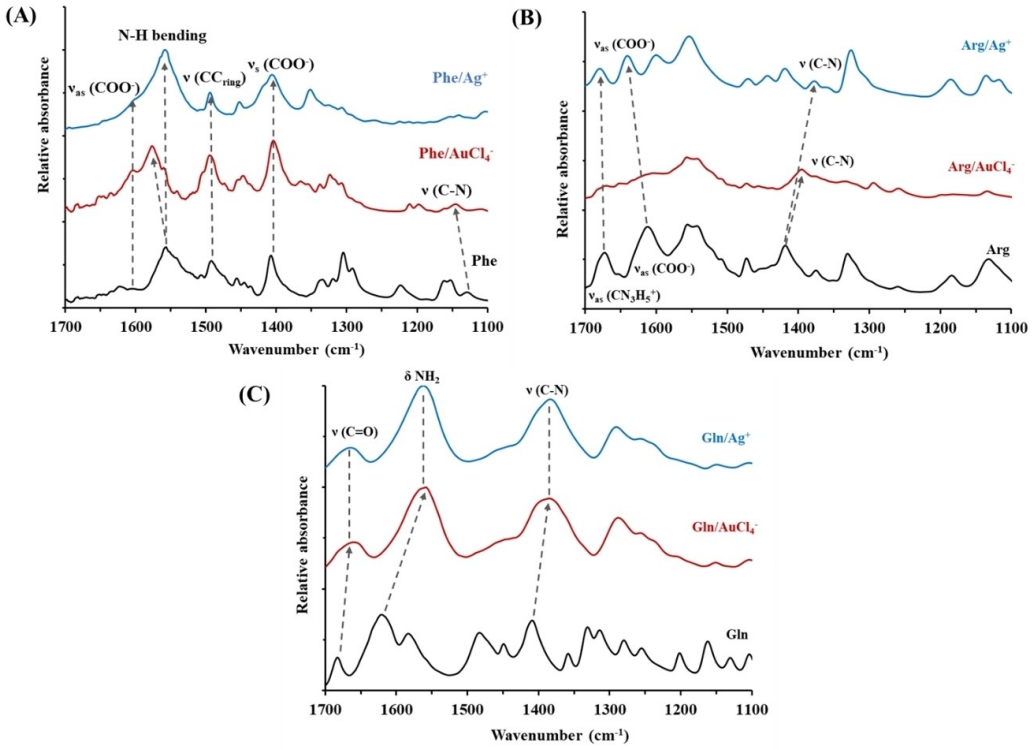

Figure 5. FTIR spectra of the pure amino acids (**A**: Phe, **B**: Arg, **C**: Gln) and the fluorescent products formed in each system at same pH conditions.

extra citrate used in the synthesis. The dominant role of the guanidium side chain in metal ion(s) binding cannot be demonstrated for either system. This experimental finding in the silver-containing system can be confirmed by previous data.[26] Namely, in the Arg-Ag^+ system each silver(I) ion is bound to one arginine molecule through carboxyl oxygen and to another nitrogen atom of amino group forming a polymeric complex, which is built up by [Ag-Arg] monomer units in a chain-like manner.[26] This binding mode is confirmed by our results as well, because the ν_s (COO^-) is shifted from 1605 to 1637 cm^{-1}, while the ν (C–N) is moved from 1413 to 1372 cm^{-1}. *In case of Gln-containing samples* (Figure 5C) the formation of Au- and Ag-based NCs is likely, because the application of extra citrate ensures the suitable reduction of the metal ions. By comparing the IR spectra of pure Gln amino acid with those of metal-containing systems, the presence of a metallic character can be confirmed in both cases. No measurable difference between the metal-containing spectra can be observed. The ν (C–N) is shifted from 1405 to 1380 cm^{-1}, while the δ NH_2 is observed at 1612 and 1560 cm^{-1} for pure Gln and Gln/metal ion systems, respectively. The characteristic vibration of ν (C=O) of the side chain is shifted from 1678 to 1663 cm^{-1}, which confirms that coordination of side chains to the noble metal ions is most dominant for Gln, in contrast with Phe and Arg.To determine the size, size distribution and zeta potential of metal NCs, dynamic light scattering studies were performed over a wide pH range. This was not possible in systems containing metal complexes and ultrasmall, few-atomic metallic NCs in individual form based on the detection limit of the DLS apparatus ($d < 1$ nm). Measurable and meaningful data could only be determined in the Au-Phe system, which is summarized in Figure 6 with photographs of the samples taken under a UV lamp. As it can be seen below pH ~3 the size of the individual clusters is less than ~1 nm and the PL intensities also show low values. Starting from pH ~4, the particle size shows an increasing trend, reaching a maximum value at pH 7–8 (d ~110 nm), and then a decreasing trend is observed when the pH is further increased for both size and PL intensities. Figure S5. presents a representative TEM image of the formed aggregates at pH = 5.5. The measured zeta potential is varied in the range of −16.5–(−18.8) mV in the pH range of 7–10. Compared to the 3 gold-containing systems, only in the case of Phe no citrate was used in the synthesis, which causes a partial aggregation of individual clusters and thus an increase in fluorescence due to the AIE phenomenon. The registered photos under UV lamp also support this observation. For Arg-Au NCs the primer size of the metallic cores is less than 1 nm, and due to the formation of a salt bridge interaction mentioned previously the individual size of the clusters cannot be measured by DLS in the range of pH 2–12. In case of Gln-Au NCs the aggregation of clusters (d ~30–32 nm) is occurred from pH ~10, below this the size is less than 1 nm. The presence of citrate in this system also help in the cluster's stabilization.

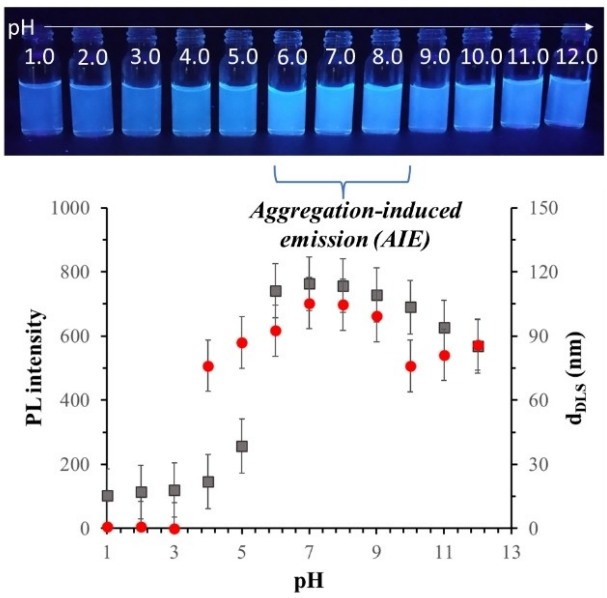

Figure 6. Hydrodynamic diameter (●) and PL intensities (■) of the NCs formed in the Au-Phe system as a function of pH with the photos of the samples.

Conclusions

Interaction of three amino acids (Phe, Arg and Gln) with $AuCl_4^-$ and Ag^+-ions have been studied at various experimental conditions to determine the effect of their molecular characteristics (type of the side chain, charge) on the possibility of the formation of fluorescent gold and silver nanoclusters. In all systems the appearance of fluorescent products having nanosecond average lifetime values was identified but we confirmed that the characteristic blue (λ_{em} = 375–460 nm) fluorescence originates from different structures depending on the side chain of the amino acids and thus their reducing capacity towards gold(III)- and silver(I)-ions. In case of Au-containing systems it was clearly confirmed that Phe > Arg > Gln is less and less suitable as a reducing ligand for the preparation of gold nanoclusters at 80 °C by using the one-step template-assisted method. However, for Arg and Gln extra use of citrate as mild reducing agent is also necessary, but the presence of citrate in the Arg-containing sample causes the detection of a relatively high QY% (~18%) which is outstanding value among the small molecule-stabilized Au NCs published in the literature so far. This outstanding value probably originates from the high Arg concentration as well as the formation of a salt bridge between the surface-located Arg and citrate. In the case of silver-containing samples only the use of Gln results in the formation of few-atomic metallic nanoclusters in presence of citrate. In contrast, by the interaction of Phe and Arg amino acids with Ag^+-ions the formation of fluorescent Ag^+-containing complexes is highly assumed instead of the appearance of nanoclusters which is confirmed by FTIR and lifetime values. Several amino acids have been studied previously for the fabrication of Au NCs to understand the formation mechanisms of the protein-templated Au NCs, thereby investigating the role of individual amino acids in the reduction process, but in case of

Phe, Arg and Glu no relevant experimental data were available in the literature. Our observations and their interpretation may contribute to better understanding the dominant role of the studied individual amino acids in template-assisted synthesis of noble metal NCs using peptides or proteins.

Experimental Section

Materials: *L*-phenylalanine (Phe, $C_9H_{11}NO_2$, ≥98%), *L*-glutamine (Gln, $C_5H_{10}N_2O_3$, ≥99%), *L*-arginine (Arg, $C_6H_{14}N_4O_2$, ≥98%), gold(III) chloride acid trihydrate ($HAuCl_4 \times 3\ H_2O$, 99.9%) were ordered from Sigma-Aldrich. Tri-sodium citrate 2-hydrate ($C_6H_5Na_3O_7 \times 2\ H_2O$, 99.7%), hydrogen chloride (HCl, 37%), sodium hydroxide (NaOH, 99%) were purchased from Molar. All chemicals were of analytical grade and were used without further purification. In all cases the stock solutions were freshly prepared using Milli-Q ultrapure water (18.2 MΩ cm^{-1} at 25 °C).

Preparation

Phe-stabilized Au nanostructures: In a first step, 10.0 mL of Phe solution at 10 mM concentration was prepared and the pH was adjusted to pH = 10.0. Secondly, 0.5 mL of a 10 mM aqueous solution of $HAuCl_4$ was added to this solution to reach the c_{Au} = 0.5 mM. This corresponds to the Phe:$[AuCl_4]^-$/20:1 molar ratio. After 24 h synthesis time the sample contains some larger aggregates, which was removed from the original dispersion by ultracentrifugation at 15,000 rpm for 60 min. The sample was further thermostated for 5 days at 80 °C. Finally, the blue-emitting dispersion was dialyzed for 24 h using a Float-A-Lyzer® G2 (MWCO = 0.1–0.5 kDa, VWR) dialysis membrane.

Phe-stabilized Ag nanostructures: Firstly, 10.0 mL of Phe solution at 60 mM concentration was prepared and the pH was adjusted to pH = 11.0. Secondly, 75.0 μL of a 100 mM aqueous solution of $AgNO_3$ was added to this solution to reach the c_{Ag} = 0.75 mM. This corresponds to the Phe:$[Ag]^+$/ 80:1 molar ratio. The sample was thermostated for 14 days at 80 °C. Finally, the small amount of precipitate formed was removed by filtration (0.2 μm syringe filter). For purification, the blue-emitting dispersion was dialyzed for 50 min using a Pur-A-Lyzer™ Mega 1000 (MWCO = 1 kDa, Sigma-Aldrich) dialysis membrane.

Arg-stabilized Au nanostructures: In the first step, 10.0 mL of Arg solution at 0.8 M concentration was prepared and the pH was adjusted to pH = 12.0. Secondly, 1.0 mL of a 10 mM aqueous solution of $HAuCl_4$ was added to this solution to reach the c_{Au} = 1.0 mM. Finally, after 5 min of continuous magnetic stirring, 5 mL of 0.01 M aqueous Na-citrate solution was added to the sample. During the synthesis Arg:$[AuCl_4]^-$/800:1 and Na-citrate:$[AuCl_4]^-$/ 5:1 molar ratio was used. The sample was monitored through 3 days continuously and every day the formed particles as well as aggregates were removed by ultracentrifugation at 15,000 rpm for 30 min. The sample was thermostated for more 8 days at 80 °C. Finally, the synthesized Arg-Au NCs were dialyzed for 50 min using a Pur-A-Lyzer™ Mega 1000 (MWCO = 1 kDa, Sigma-Aldrich) dialysis membrane.

Arg-stabilized Ag nanostructures: Firstly, 10.00 mL of Arg solution at 0.90 M concentration was prepared and the pH was adjusted to pH = 12.0. Secondly, 0.153 mL of a 100 mM aqueous solution of $AgNO_3$ was added to this solution to adjust the c_{Ag} = 1.5 mM. During the synthesis Arg:$[Ag]^+$/ 600:1 molar ratio was applied. The sample was thermostated for 6 days at 80 °C. Finally, the small amount of precipitate formed was removed by filtration (0.2 μm syringe filter). The synthesized Arg-Ag NCs were dialyzed for 80 min using a Pur-A-Lyzer™ Mega 1000 (MWCO = 1 kDa, Sigma-Aldrich) dialysis membrane.

Gln-stabilized Au nanostructures: 10.0 mL of Gln solution at 0.25 M concentration was prepared and mixed with 0.4 mL of 2.5 M aqueous Na-citrate solution and the pH was adjusted to pH = 6.0. Secondly, 1 mL of a 10 mM aqueous solution of $HAuCl_4$ was added to this mixture, where the final metal concentration was c_{Au} = 1 mM. During the synthesis Gln:$[AuCl_4]^-$/250:1 and Na-citrate:$[AuCl_4]^-$/100:1 molar ratio was used. After 24 h, the sample contains large number of colloidal particles/aggregates, which was removed from the dispersion by ultracentrifugation at 15,000 rpm for 30 min. The sample was further thermostated for 6 days at 80 °C. Finally, the synthesized Gln-Au NCs were dialyzed for 40 min using a Pur-A-Lyzer™ Mega 1000 (MWCO = 1 kDa, Sigma-Aldrich) dialysis membrane.

Gln-stabilized Ag nanostructures: 8.750 mL of a 0.4 M aqueous Gln solution was mixed with 1.12 mL of 2.5 M aqueous Na-citrate solution, and the initial pH was adjusted to pH = 6.0 and 0.1 mL of a 100 mM aqueous solution of $AgNO_3$ was added to this solution to adjust the c_{Ag} = 1 mM. During the synthesis Gln:$[Ag]^+$/350:1 and Na-citrate:$[Ag]^+$/ 280:1 molar ratio was kept constant. The sample was thermostated for 14 days at 80 °C. The small amount of precipitate formed was removed by filtration (0.2 μm syringe filter). Finally, the synthesized Gln-Ag NCs were dialyzed for 20 min using a Pur-A-LyzerTM Mega 1000 (MWCO = 1 kDa, Sigma-Aldrich) dialysis membrane.

Methods of characterization

Optical characteristic: The optical characterization was performed on an ABL&E JASCO FP-8500 spectrofluorometer using a 4-sided quartz cuvette with 1 cm optical length. The excitation and emission spectra were recorded by using 2.5–2.5 nm bandwidths, 200 nm/min scan speed, and 1 nm resolution. The absolute internal quantum yield (QY%) was calculated based on the incident light spectra, the indirect and direct excitation of the samples in 2 mm optical length on the same apparatus equipped with the ABL&E JASCO ILF-835 integrating sphere. For the calibration, an ABL&E JASCO ESC-842 calibrated WI light source was used, therefore, other references were not necessary. For the calculation SpectraManager 2.0 software of the instrument was used for calculations. Fluorescence lifetime was determined by time-correlated single photon counting (TCSPC) on a Horiba DeltaFlex device equipped with a DeltaDiode pulsed laser (λ_{laser} = 371 nm) or LED (λ_{LED} = 310 nm) light sources depending on the sample in a 1 cm quartz cuvette. The emitted lights were detected at the wavelength of

maximum emission intensity. The number of counts on the peak channel was 10000 and to determine the instrument response function (IRF), standard SiO_2 colloids (LUDOX® TM-50 colloidal silica, Sigma) was applied. The calculation of the main lifetime components was done by the exponential fitting of decay curves in the EZTime measurement and analysis program of Horiba. The χ^2 values represent the goodness of the fitting.

Structural characteristic: FTIR spectra of the pure amino acids in powder form and the lyophilized amino acid-directed fluorescent Au and Ag products were registered on a BIO-RAD Digilab Division FTS-65 A/896 Fourier Transform infrared spectrometer with a Harrick's Meridian® SplitPea single-reflection diamond attenuated total reflectance (ATR) accessory. All IR spectra were recorded at 4 cm^{-1} optical resolution by averaging 256 interferograms. The pH of the amino acid powders and the Au- and Ag-based products was same. The stability and thus the size and Zeta-potential values of the fluorescent nano-objects were studied on a Malvern Zetasizer NanoZS ZEN 4003 apparatus equipped with a He–Ne laser ($\lambda = 633$ nm) at 25 ± 0.1 °C. The ionic strength was regulated by 0.1 M NaCl, and the hydrodynamic diameters (d_H) were calculated by the Smoluchowski model. Transmission electron microscopy (TEM) images were recorded on a FEI Tecnai G2 instrument at 200 kV accelerating voltage and the pictures were analyzed using ImageJ open-access software. To check the reducing capability of the studied amino acids and to confirm the formation of clusters, simple ion reactions using KI were performed. Unreduced Ag^+ ions can be identified as a yellowish precipitate of AgI, while the partially reduced gold(III) ions (as gold(I)ions) can be detected as a red complex of gold(I)iodide (AuI_2^-) under the influence of iodide.

Acknowledgements

The research was supported by the National Research, Development, and Innovation Office-NKFIH through the PD137938 and FK131446 projects. Project no. TKP2021-EGA-32 has been implemented with the support provided by the Ministry of Innovation and Technology (MIT) of Hungary from the National Research, Development and Innovation Fund (NRDIF), financed under the TKP2021-EGA funding scheme. Ditta Ungor gratefully appreciates the financial support of the János Bolyai Research Scholarship of the Hungarian Academy of Sciences.

Conflict of Interests

The authors declare no conflict of interest.

Data Availability Statement

The data that support the findings of this study are available from the corresponding author upon reasonable request.

Keywords: amino acids · fluorescence · gold nanoclusters · quantum yield · silver complexes

[1] K. Saha, S. S. Agasti, C. Kim, X. Li, V. M. Rotello, *Chem. Rev.* **2012**, *112*, 2739–2779.
[2] W. Zhou, X. Gao, D. Liu, X. Chen, *Chem. Rev.* **2015**, *115*, 10575–10636.
[3] Y. Du, H. Sheng, D. Astruc, M. Zhu, *Chem. Rev.* **2020**, *120*, 526–622.
[4] D. Ungor, I. Dékány, E. Csapó, *Nanomater.* **2019**, *9*, 1229.
[5] A. Czyżowska, A. Barbasz, L. Szyk-Warszyńska, M. Oćwieja, E. Csapó, D. Ungor, *Colloids Surf. A* **2021**, *620*, 126569.
[6] V. Hornok, E. Csapó, N. Varga, D. Ungor, D. Sebők, L. Janovák, G. Laczkó, I. Dékány, *Colloid Polym. Sci.* **2016**, *294*, 49–58.
[7] D. Ungor, K. Horváth, I. Dékány, E. Csapó, *Sens. Actuators B* **2019**, *288*, 728–733.
[8] E. Csapó, D. Ungor, Á. Juhász, G. K. Tóth, I. Dékány, *Colloids Surf. A* **2016**, *511*, 264–271.
[9] Y. Wang, Y. Tan, Y. Ding, L. Fu, W. Qing, *Colloids Surf. A* **2022**, *654*, 130072.
[10] S. Bhunia, K. Gangopadhyay, A. Ghosh, S. K. Seth, R. Das, P. Purkayastha, *ACS Appl. Nano Mater.* **2021**, *4*, 305–312.
[11] M. R. Mahmoudian, W. J. Basirun, P. M. Woi, R. Yousefi, Y. Alias, *Anal. Bioanal. Chem.* **2019**, *411*, 517–526.
[12] Z. Wei, Y. Pan, G. Hou, X. Ran, Z. Chi, Y. He, Y. Kuang, X. Wang, R. Liu, L. Guo, *ACS Appl. Mater. Interfaces.* **2022**, *14*, 2452–2463.
[13] A. Amiri-Sadeghan, A. Dinari, S. Mohammadi, T. Zohrabi, R. Khodarahmi, S. Hosseinkhani, J. Yoon, *Sci. Rep.* **2022**, *121(12)*, 1–10.
[14] D. Ungor, E. Csapó, B. Kismárton, A. Juhász, I. Dékány, *Colloids Surf. B* **2017**, *155*, 35–141.
[15] E. Canel, A. Gültepe, A. Doğan, E. Kilıç, *J. Solution Chem.* **2006**, *35*, 5–19.
[16] X. Mu, L. Qi, P. Dong, J. Qiao, J. Hou, Z. Nie, H. Ma, *Biosens. Bioelectron.* **2013**, *49*, 249–255.
[17] K. T. Chan, G. S. M. Tong, W. P. To, C. Yang, L. Du, D. L. Phillips, C. M. Che, *Chem. Sci.* **2017**, *8*, 2352–2364.
[18] E. E. Langdon-Jones, D. Lloyd, A. J. Hayes, S. D. Wainwright, H. J. Mottram, S. J. Coles, P. N. Horton, S. J. A. Pope, *Inorg. Chem.* **2015**, *54*, 6606–6615.
[19] D. M. Wood, N. W. Ashcroft, *Phys. Rev. B.* **1982**, *25*, 6255.
[20] D. Cheng, R. Liu, K. Hu, *Front. Chem.* **2022**, *10*, 861.
[21] J. Zheng, C. Zhou, M. Yu, J. Liu, Different sized luminescent gold nanoparticles, Nanoscale **2012**, 4 4073–4083.
[22] K. Pyo, V. D. Thanthirige, K. Kwak, P. Pandurangan, G. Ramakrishna, D. Lee, *J. Am. Chem. Soc.* **2015**, *137*, 8244–8250.
[23] T. Q. Yang, B. Peng, B. Q. Shan, Y. X. Zong, J. G. Jiang, P. Wu, K. Zhang, *Nanomater.* **2020**, *10*, 261.
[24] Y. Huang, L. Fuksman, J. Zheng, *Dalton Trans.* **2018**, *47*, 6267–6273.
[25] N. C. Polfer, J. Oomens, D. T. Moore, G. Von Helden, G. Meijer, R. C. Dunbar, *J. Am. Chem. Soc.* **2006**, *128*, 517–525.
[26] S. Ahmad, A. Yousaf, M. N. Tahir, A. A. Isab, M. Monim-Ul-Mehboob, W. Linert, M. Saleem, *J. Struct. Chem.* **2015**, *56*, 1653–1657.

Manuscript received: March 6, 2023
Accepted manuscript online: May 31, 2023
Version of record online: July 18, 2023